OTC 4309

On the Dynamic Analysis of Multi-Component Mooring Lines

by Toshio Nakajima, *Sumitomo Heavy Industries Ltd.*, and Seizo Motora and Masataka Fujino, *University of Tokyo*

This paper was presented at the 14th Annual OTC in Houston, Texas, May 3-6, 1982. The material is subject to correction by the author. Permission to copy is restricted to an abstract of not more than 300 words.

ABSTRACT

This paper presents the results of both theoretical and experimental studies on the dynamic tensions and motions of the multi-component mooring lines such as chain with clump weights and/or spring buoys. Especially, the author's attention is paid to analysis of the dynamic behavior of a mooring line under the excitation caused by the motion of floating platform.

Appearance of new types of multi-component mooring lines demands the development of numerical methods which are able to be applied for the analysis of dynamic behavior of various types of mooring lines. In this paper a new method is proposed by the authors, which is motivated by the lumped mass method originally developed by Walton and Polachek (1959). The present method, however, is somewhat modified to be applied to the analysis of the multi-component mooring system and extended to be able to include the elastic deformation of the mooring line.

The time histories of dynamic tension predicted by the present method are compared with the experimentanl ones with excellent agreement.

INTRODUCTION

In recent years, ocean platforms have become more and more complex and at the same time the requirement of the mooring systems used for those platforms becomes more severe. For use as these mooring systems, the mooring lines with a combination of chains and wire ropes, and those connected with buoys and/or clump weights have come to be used.

Since the dynamic behaviors of those mooring lines are complicated and somewhat different from those of conventional single lines, the dynamic analysis of those lines become more important for investigating the feasibility and safety of mooring of the floating platforms.

For this study, a new method of the non-linear dynamic analysis of multi-component mooring lines is developed to obtain a better understanding of the dynamic behavior of multi-component mooring lines. In the present method, the continuous distribution of the mooring line's mass replaced by a discrete distribution of lumped masses at a finite number of points on the line. This replacement amounts to idealizing the system as a set of point masses and non-mass linear springs. At the present analysis, non-linearities of viscous damping acting on the mooring line are considered.

The present method has a great potential of application for engineers as it does not require lengthy procedure of numerical calculation and it can save a good deal of computing time. One average run over 4 cycles of harmonic motion may (240 time steps) require approximalety 10 seconds in the case of the mooring line model of 9 segments by using IBM 3033. For example;

GOVERNING EQUATIONS OF MOTION

First, a mooring line is represented by a set of discrete masses interconnected by springs as illustrated in Fig. 1. The external forces acting on a mooring line are gravity, hydrodynamic forces and line tension.

The governing equations of motion of j-th lumped mass are as follows;

$$[M_j + A_{nj} \sin^2\bar{\gamma}_j + A_{tj} \cos^2\bar{\gamma}_j]\cdot\ddot{x}_j + [A_{tj}-A_{nj}]\cdot\ddot{z}_j \sin\bar{\gamma}_j \cos\bar{\gamma}_j = F_{xj} \quad \ldots\ (1)$$

$$[M_j + A_{nj} \cos^2\bar{\gamma}_j + A_{tj} \sin^2\bar{\gamma}_j]\cdot\ddot{z}_j + [A_{tj}-A_{nj}]\cdot\ddot{x}_j \sin\bar{\gamma}_j \cos\bar{\gamma}_j = F_{zj} \quad \ldots\ (2)$$

$$(j=2,3, \ldots, N)$$

where

M_j, A_{nj}, A_{tj} : Mass of j-th lump, and its added masses in normal and tangential directions respectively.

$\ddot{x}_j$, $\ddot{z}_j$: Accelerations of j-th lumped mass in x and z directions respectively.

The nodal components of the external forces F_{xj} and F_{zj} in Eq. (1) and Eq. (2) can be written by

$$F_{xj} = T_j \cos \gamma_j - T_{j-1} \cos \gamma_{j-1} - f_{dxj} \quad \ldots\ldots (3)$$

$$F_{zj} = T_j \sin \gamma_j - T_{j-1} \sin \gamma_{j-1} - f_{dzj} - \delta_j \quad \ldots\ldots (4)$$

where

T_j : Tension in a segment between j-th and (j+1)-th lumped masses

δ_j : weight in water of lumped mass

It is assumed that the drag force action on the mooring line is proportional to the square of fluid velocity relative to mooring line.

$$f_{dxj} = -\frac{\rho}{2} D_c \bar{\ell} [C_{dn} \sin \bar{\gamma}_j |u_{nj}| u_{nj} - C_{dt} \cos \bar{\gamma}_j |u_{tj}| u_{tj}] + \frac{\rho}{2} A_{rx} C_{dx} |\dot{x}_j - c_j| (\dot{x}_j - c_j) * \quad \ldots\ldots (5)$$

$$f_{dzj} = \frac{\rho}{2} D_c \bar{\ell} [C_{dn} \cos \bar{\gamma}_j |u_{nj}| u_{nj} + C_{dt} \sin \bar{\gamma}_j |u_{tj}| u_{tj}] + \frac{\rho}{2} A_{rz} C_{dz} |\dot{z}_j| \dot{z}_j * \quad \ldots\ldots (6)$$

(j=2, 3, ...N)

where

D_c : equivalent diameter of mooring line

$\bar{\ell}$: original length of line segment

ρ : density of water

C_{dn}, C_{dt} : coefficients of drag forces normal and tangential to the mooring line respectively.

---

* In addition to the drag on the line itself, there will also be hydrodynamic drag on any concentrated substances attached to the mooring line such as spring buoy and clump weight.

A_{rx}, A_{rz} : projected area of the additional concentrated substances such as spring buoy in x and z directions respectively.

C_{dx}, C_{dz} : drag coefficients of the additional concentrated substances in x and z directions respectively.

The velocity components u_{nj} and u_{tj} normal and tangential to the mooring line are given by

$$u_{nj} = -(\dot{x}_j - c_j) \sin \gamma_j + \dot{z}_j \cos \gamma_j \quad \ldots\ldots (7)$$

$$u_{tj} = (\dot{x}_j - c_j) \cos \gamma_j + \dot{z}_j \sin \gamma_j \quad \ldots\ldots (8)$$

where c_j is the current velocity in horizontal direction at j-th lumped mass.

The additional constraint equation of the mooring line is

$$(x_j - x_{j-1})^2 + (z_j - z_{j-1})^2 = \bar{\ell}^2 \left(1. + \frac{T_{j-1}}{A \cdot E}\right)^2 \quad \ldots\ldots (9)$$

(j=2, 3, ..., N+1)

where

A : cross-sectional area of line
E : modulus of elasticity

SOLUTION OF THE PROBLEM

The govening equations (1) and (2) can be reduced to:

$$\ddot{x}_j = (R_j T_j - P_j T_{j-1} + U_j)/\Delta t^2 \quad \ldots\ldots (10)$$

$$\ddot{z}_j = (S_j T_j - Q_j T_{j-1} + V_j)/\Delta t^2 \quad \ldots\ldots (11)$$

(j=2, 3 ...N)

where

$$I_1 = M_j + A_{nj} \sin^2 \bar{\gamma}_j + A_{tj} \cos^2 \bar{\gamma}_j$$

$$I_2 = [A_{tj} - A_{nj}] \sin \bar{\gamma}_j \cos \bar{\gamma}_j$$

$$I_3 = M_j + A_{nj} \cos^2 \bar{\gamma}_j + A_{tj} \sin^2 \bar{\gamma}_j$$

$$R_j = \Delta t^2 [I_3 \cdot \cos \bar{\gamma}_j - I_2 \cdot \sin \bar{\gamma}_j]/\lambda$$

$$P_j = \Delta t^2 [I_3 \cdot \cos \bar{\gamma}_{j-1} - I_2 \cdot \sin \bar{\gamma}_{j-1}]/\lambda$$

$$S_j = \Delta t^2 [I_1 \cdot \sin \bar{\gamma}_j - I_2 \cdot \cos \bar{\gamma}_j]/\lambda$$

$$Q_j = \Delta t^2 [I_1 \cdot \sin \bar{\gamma}_{j-1} - I_2 \cdot \cos \bar{\gamma}_{j-1}]/\lambda$$

$$U_j = \Delta t^2 [I_2 (f_{dzj} + \delta_j) - I_3 \cdot f_{dxj}]/\lambda$$

$$V_j = \Delta t^2 [I_2 \cdot f_{dxj} - I_1 (f_{dzj} + \delta_j)]/\lambda$$

$$\lambda = I_1 \cdot I_3 - I_2^2 \quad \ldots\ldots (12)$$

On the other hand, the nodal accelerations and velocities of the next time step ($\ddot{x}_j^{n+1}$, $\ddot{z}_j^{n+1}$), ($\dot{x}_j^{n+1}$, $\dot{z}_j^{n+1}$) can be expressed by the following finite-difference equations so called Houbolt Method.

$$\ddot{s}_j^{n+1} = \frac{1}{\Delta t^2}(2 s_j^{n+1} - 5 s_j^n + 4 s_j^{n-1} - s_j^{n-2}) \quad \cdots\cdots(13)$$

$$\dot{s}_j^{n+1} = \frac{1}{6\Delta t}(11 s_j^{n+1} - 18 s_j^n + 9 s_j^{n-1} - 2 s_j^{n-2}) \quad \cdots\cdots(14)$$

where a dot over s_j denotes time differentiation and s_j in equations (13) and (14) represents x_j or z_j.

Combining equations (10), (11) and (13), the nodal displacements x_j^{n+1} and z_j^{n+1} of next time step n+1 are derived as follows:

$$x_j^{n+1} = \frac{5}{2} x_j^n - 2 x_j^{n-1} + \frac{1}{2} x_j^{n-2} + (R_j^{n+1}\cdot T_j^{n+1} - P_j^{n+1}\cdot T_{j-1}^{n+1} + U_j^{n+1})/2 \quad \cdots(15)$$

$$z_j^{n+1} = \frac{5}{2} z_j^n - 2 z_j^{n-1} + \frac{1}{2} z_j^{n-2} + (S_j^{n+1}\cdot T_j^{n+1} - Q_j^{n+1}\cdot T_{j-1}^{n+1} + V_j^{n+1})/2 \quad \cdots(16)$$

To obtain the tensions of next time step T_j^{n+1}, we use the Newton-Raphson Method. It is assumed that T_j^{n+1} consists of two components as follows:

$$T_j^{n+1} = \tilde{T}_j^{n+1} + \Delta T_j^{n+1} \quad \cdots\cdots(17)$$

where $\tilde{T}_j^{n+1}$ is the tentative value of the tension and ΔT_j^{n+1} is the correction.

Now, we define the following equation which is a function of line tension of next time step. This equation is derived from Eq. (9).

$$\psi_j^{n+1} = -\bar{\ell}^2(1+T_{j-1}^{n+1}/E\cdot A)^2 + (x_j^{n+1} - x_{j-1}^{n+1})^2 + (z_j^{n+1} - z_{j-1}^{n+1})^2 = \psi_j^{n+1}(T_{j-2}^{n+1}, T_{j-1}^{n+1}, T_j^{n+1}) = 0 \quad \cdots\cdots(18)$$

$$(j=2, 3 \ldots N)$$

Expanding ψ_j^{n+1} in a Taylor series about the $\{\tilde{T}_{j-2}^{n+1}, \tilde{T}_{j-1}^{n+1}, \tilde{T}_j^{n+1}\}$, thus we obtain

$$\psi_j^{n+1} = \tilde{\psi}_j^{n+1} + \frac{\partial\tilde{\psi}_j^{n+1}}{\partial T_{j-2}^{n+1}}\cdot\Delta T_{j-2}^{n+1} + \frac{\partial\tilde{\psi}_j^{n+1}}{\partial T_{j-1}^{n+1}}\cdot\Delta T_{j-1}^{n+1} + \frac{\partial\tilde{\psi}_j^{n+1}}{\partial T_j^{n+1}}\cdot\Delta T_j^{n+1} + (\text{Higher order terms}) = 0 \quad \cdots\cdots(19)$$

Provided that the tentative values $\tilde{T}_j^{n+1}$ are sufficiently close to the correct values T_j^{n+1}, we may neglect the higher order terms in Eq. (19), and thereby obtain a system of N linear equations for the differential correction ΔT_j^{n+1}.

$$\tilde{E}_j^{n+1}\cdot\Delta T_{j-2}^{n+1} - \tilde{F}_j^{n+1}\cdot\Delta T_{j-1}^{n+1} + \tilde{G}_j^{n+1}\cdot\Delta T_j^{n+1} = -\tilde{\psi}_j^{n+1} \quad \cdots\cdots(20)$$

$$(j=2, 3 \ldots, N+1)$$

where

$$\tilde{\psi}_j^{n+1} = -\bar{\ell}^2(1+\tilde{T}_{j-1}^{n+1}/E\cdot A)^2 + (\tilde{x}_j^{n+1} - \tilde{x}_{j-1}^{n+1})^2 + (\tilde{z}_j^{n+1} - \tilde{z}_{j-1}^{n+1})^2 \quad \cdots\cdots(21)$$

$$\tilde{E}_j^{n+1} = \frac{\partial\tilde{\psi}_j^{n+1}}{\partial T_{j-2}^{n+1}} = \tilde{P}_{j-1}^{n+1}(\tilde{x}_j^{n+1} - \tilde{x}_{j-1}^{n+1}) + \tilde{Q}_{j-1}^{n+1}(\tilde{z}_j^{n+1} - \tilde{z}_{j-1}^{n+1}) \quad \cdots\cdots(22)$$

$$\tilde{F}_j^{n+1} = -\frac{\partial\tilde{\psi}_j^{n+1}}{\partial T_{j-1}^{n+1}} = (\tilde{P}_j^{n+1} + \tilde{R}_{j-1}^{n+1})(\tilde{x}_j^{n+1} - \tilde{x}_{j-1}^{n+1}) + (\tilde{Q}_j^{n+1} + \tilde{S}_{j-1}^{n+1})(\tilde{z}_j^{n+1} - \tilde{z}_{j-1}^{n+1}) + 2\bar{\ell}^2(1 + \tilde{T}_{j-1}^{n+1}/E\cdot A)/E\cdot A \quad \cdots\cdots(23)$$

$$\tilde{G}_j^{n+1} = \frac{\partial\tilde{\psi}_j^{n+1}}{\partial T_j^{n+1}} = \tilde{R}_j^{n+1}(\tilde{x}_j^{n+1} - \tilde{x}_{j-1}^{n+1}) + \tilde{S}_j^{n+1}(\tilde{z}_j^{n+1} - \tilde{z}_{j-1}^{n+1}) \quad \cdots\cdots(24)$$

$$(j=2, 3, \ldots N+1)$$

and

$$\tilde{x}_j^{n+1} = \frac{5}{2} x_j^n - 2x_j^{n-1} + \frac{1}{2} x_j^{n-2} + [\tilde{R}_j^{n+1}\tilde{T}_j^{n+1} - \tilde{P}_j^{n+1}\tilde{T}_{j-1}^{n+1} + \tilde{U}_j^{n+1}]/2 \quad \cdots\cdots(25)$$

$$\tilde{z}_j^{n+1} = \frac{5}{2} z_j^n - 2z_j^{n-1} + \frac{1}{2} z_j^{n-2} + [\tilde{S}_j^{n+1} \cdot \tilde{T}_j^{n+1} - \tilde{Q}_j^{n+1} \cdot \tilde{T}_{j-1}^{n+1} + \tilde{V}_j^{n+1}]/2 \quad (j=2,3, \ldots N) \quad \ldots\ldots(26)$$

where $\tilde{R}_j^{n+1}$, $\tilde{S}_j^{n+1}$, $\tilde{P}_j^{n+1}$, $\tilde{Q}_j^{n+1}$, $\tilde{V}_j^{n+1}$, $\tilde{U}_j^{n+1}$ are the tentative values of R_j^{n+1}, S_j^{n+1}, P_j^{n+1}, V_j^{n+1}, U_j^{n+1} in equations (12).

COMPUTATIONAL PROCEDURES

The computational procedures of solving the dynamic behavior of mooring lines are as follows:

1) Calculate the equilibrium form and tensions of mooring line when the line is in a static equilibrium. The mathematical formulation of static calculation by the lumped mass model is described in Ref. 3 and Ref. 5.

2) The oscillation at the upper end P $(x_{N+1}^{n+1}, z_{N+1}^{n+1})$ of the mooring line is assumed to start from rest and gradulaly approach a sinusoidal motion in accordance with the following equations:

$$x_{N+1}^{n+1} = x_{N+1}^0 + (1. - e^{-\nu t}) \cdot A_p \cdot \sin(\omega t + \varepsilon_x) \quad \ldots\ldots(27)$$

$$z_{N+1}^{n+1} = z_{N+1}^0 + (1. - e^{-\nu t}) \cdot B_p \cdot \sin(\omega t + \varepsilon_z) \quad \ldots\ldots(28)$$

where

$\nu, \varepsilon_x, \varepsilon_z$: chosen parameters

ω : frequency of motion

t : time [$= (n+1) \cdot \Delta t$]

A_p, B_p: amplitude of motion in x and z directions respectively.

3) Correct the weights of the lumped masses nearest to the bottom by the equations described in Appendix.

4) Calculate the matrix coefficients $\tilde{R}_j^{n+1}$, $\tilde{S}_j^{n+1}$, $\tilde{P}_j^{n+1}$, $\tilde{Q}_j^{n+1}$.

5) Calculate the drag forces acting on the line due to the tentative velocities $\tilde{\dot{x}}_j$, $\tilde{\dot{z}}_j$.

6) Calculate tensions of the next time step T_j^{n+1} by iteration. In this step, the tensions of previous time step T_j^n is used for the first approximation of the tentative values $\tilde{T}_j^{n+1}$. Then, we determine the corrections ΔT_j^{n+1} by the following equation derived from Eq. (20).

$$\begin{bmatrix} \Delta T_1^{n+1} \\ \Delta T_2^{n+1} \\ \vdots \\ \Delta T_N^{n+1} \end{bmatrix} = \begin{bmatrix} -\tilde{F}_2^{n+1} & \tilde{G}_2^{n+1} & & \\ \tilde{E}_3^{n+1} & -\tilde{F}_3^{n+1} & \tilde{G}_3^{n+1} & \\ & \ddots & \ddots & \ddots \\ & & \tilde{E}_{N+1}^{n+1} & -\tilde{F}_{N+1}^{n+1} \end{bmatrix}^{-1} \cdot \begin{bmatrix} -\tilde{\Psi}_2^{n+1} \\ -\tilde{\Psi}_3^{n+1} \\ \vdots \\ -\tilde{\Psi}_{N+1}^{n+1} \end{bmatrix} \quad \ldots(29)$$

7) Calculate the nodal displacements of the next time step (x_j^{n+1}, z_j^{n+1}) by Eqs. (15) and (16).

8) The iterative procedure from step 4) to step 7) is continued until the appropriate convergence is attained.

9) Repeat the calculational procedure from step 2), as time step changes from n to n+1.

EXPERIMENTS

Tank tests have been performed with models of single and multiple-component mooring chains. The multiple-component mooring chains used at the experiments are of three kinds such as

1) chain with 180ϕ spherical spring buoy (of styrol form)

2) chain with 226ϕ spherical spring buoy (of wood)

3) chain with clump weight (of lead)

The principal particulars of the chain are shown in Table 1 while those of spring buoys and clump weight are summerized in Table 2.

Material		Steel (without stud)
Weight per Length in water	W_w	0.1938 kg/m
in air	W_A	0.222 kg/m
Equivalent Diameter	D_c	0.599 cm
Volume per Length		28.2 cm^3/m
Modulus of elasticity		2.15 x 10^6 kg/cm^2

Table 1 Principal Particulars of Chain

	Spring Buoy (B1 buoy)	Spring Buoy (B2 buoy)	Clump Weight
Material	Styrol Form	Wood	Lead
Diameter	18.0 cm	22.6 cm	7.5 cm
Weight in air	0.07 kg	4.1 kg	2.0 kg
Weight in water or Buoyancy Force	-3.0 kg	-1.9 kg	1.823 kg

Table 2 Principal Particulars of Spring Buoys and Clump Weight

Forced oscillation tests of the mooring chains described above were carried out in calm water. The lower end of chain was attached rigidly to the bottom of the model basin and the upper end attached to a mechanical oscillator was forced to oscillate horizontally with amplitude A_p = 5 cm (See Fig. 2). The driving mechanism of oscillating the chain is shown in Photo. 1. It is essentially a crank-type device with a drive rod.

The horizontal and vertical tensions are measured by load cell (shown as Block Gauge) located at the upper end as shown in Fig. 3 while the tension at the anchored point is measured by a ring gauge.

COMPARISON BETWEEN THEORETICAL AND EXPERIMENTAL RESULTS

At the numerical calculation of dynamic behavior of a single mooring line, the total length of the line was divided into 9 segments of equal length, while the multi-component mooring lines were represented by 16 segments (See Fig. 4). The time increment Δt was equal to 0.02 seconds in both cases of single and multi-component mooring lines.

The hydrodynamic coefficients of mooring line such as added mass coefficients (C_{hn}, C_{ht}) and viscous damping coefficients (C_{dn}, C_{dt}) used for the numerical computation are obtained by experiments and are as follows:

C_{hn} (added mass in normal dir./$\rho D_c^2 \pi \bar{\ell}/4$) = 1.98

C_{ht} (added mass in tangential dir./$\rho D_c^2 \pi \bar{\ell}/4$) = 0.2

C_{dn} (drag force in normal dir./ $\frac{4}{3\pi}\rho \cdot D_c \cdot \bar{\ell}\, u_n^2$) = 2.18

C_{dt} (drag force in tangential dir./ $\frac{4}{3\pi}\rho \cdot D_c \cdot \bar{\ell} \cdot u_t^2$) = 0.17

Fig. 5 shows the time histories of vertical and horizontal components of tension at the mooring point P in the case where the point P was oscillated harmonically in the horizontal direction. Comparing the predicted time histories with those measured at the experiments for various number of periods of motion T, it is concluded that the predicted values agree well with the measured ones quantitavily. Therefore, it is considered that the present method is useful for dynamic analysis of the mooring line.

The frequency response curves of tension are plotted against the non-dimensional frequency in Fig. 6. The amplitudes of horizontal and vertical components of tension, T_H and T_V respectively, are non-dimensionalized by dividing with T_{HO} and T_{VO} which denote the horizontal and vertical components of tension at the static equilibrium state with null displacement of the point P. It should be noted that the tension increases with the frequency of motion and becomes significant to cause failure at higher frequency. Fig. 7 shows the difference of the predicted amplitudes T_H and T_V at the point P which are brought about by changing the coefficient C_{dn} of hydrodynamic drag acting on the normal direction of the mooring line. It is evident that the higher the damping coefficient is, the greater the amplitudes of the dynamic tension are.

The comparisons between theoretical and experimental results for the mooring chains with spring buoy are also made and shown in Fig. 8. As shown in Fig. 8, a spring buoy of which the weight in the water is equal to - 3 kg (- means that the buoyant force exceeds the gravity force) is attached to the mooring line at the center of the line. The frequency response curves of the dynamic tension of the mooring line with spring buoys are shown in Fig. 9.

Comparing the values of tension of the mooring chain with a spring buoy with those of single mooring chain, it is evident that the buoy is extremely effective in decreasing the dynamic tension of chain. The motions of the mooring chain and spring buoy are plotted in Fig. 10.

Finally, the time-domain simulation of the mooring chain with clump weight is executed and the results are shown in Fig. 11. Again, good agreement between theoretical and experimental results is obtained. Both results show that impact load of chain appears when the clump weight is lifted up from the bottom of the water, while the drastic change of tension occurs as the clump weight hit the bottom.

CONCLUDING REMARKS

Dynamic behaviors of the various multi-component mooring lines are investigated theoretically and experimentally, and in consequence, it is clarified that the behaviors of the multi-component mooring line are complicated and somewhat different from those of the conventional single mooring line. Other results obtained are as follows:

1) At higher frequencies, the dynamic tension is significant and may be of magnitude sufficient to cause a failure.

2) Spring buoy exhibits larger motions and causes the "wear and tear" problem between buoy and mooring line while magnitude of the dynamic tension of line is small.

3) Clump weight affects the line tension of mooring line considerably. Especially, the lift-up of the clump weight from the bottom causes a remarkable increase of the dynamic tension of the mooring line.

In conclusion, it is shown that the present lumped mass method provides a realistic representation of the dynamics of mooring line and is applicable to numerical analysis of multi-component mooring lines without tremendous computing time.

NOMENCLATURE

A	:	cross-sectional area of mooring line
A_{nj}, A_{tj}	:	added masses of j-th line segment in normal and tangential directions respectively
A_{rx}, A_{rz}	:	projected Area of the additional concentrated substances in x and z directions respectively
A_p, B_p	:	amplitudes of motion in x and z directions respectively
c_j	:	current velocity at j-th lumped mass
C_{hn}, C_{ht}	:	added mass coefficients of mooring line in normal and tangential directions respectively
C_{dn}, C_{dt}	:	damping coefficients of mooring line in normal and tangential directions respectively

C_{dx}, C_{dz} : damping coefficients of the additional concentrated substances in x and z directions respectively

D_c : equivalent diameter of mooring line

E : modulus of elasticity

F_{xj}, F_{zj} : nodal components of external forces in x and z directions respectively

f_{dxj}, f_{dzj} : nodal components of drag forces in x and z directions respectively

g : gravity accerelation

L : total length of mooring line

$\bar{\ell}$: original length of line segment

M_j : mass of j-th lump (virtual mass of the additional concentrated substances will be included in M_j)

N : number of line segment (number of lumped masses is (n-1))

T : period of motion

$T_j(T_j^{n+1})$: line tension in segment between j-th and (j+1)-th lumped mass

ΔT_j^{n+1} : correction of tentative tension $\tilde{T}_j^{n+1}$

T_H, T_V : amplitudes of dynamic tension at the mooring point P in horizontal and vertical directions respectively

T_X, T_Z : line tensions at the mooring point P in x and z directions respectively

T_{HO}, T_{VO} : pre-tensions at the mooring point P in horizontal and vertical directions respectively

t : time [$n\cdot\Delta t$] ($n = 0, 1, 2, \ldots\ldots$)

Δt : time increment

u_{nj}, u_{tj} : velocity components of j-th lumped mass in normal and tangential directions respectively

W_w, W_A : weights of mooring line per length in water and in air respectively

W_c : weight of mooring line segment ($= W_w\cdot\bar{\ell}$)

x_j, z_j (x_j^{n+1}, z_j^{n+1}) : displacements of j-th lumped mass in x and z directions respectively

δ_j : weight of j-th lumped mass in water

ρ : density of water

ω : frequency of motion

ACKNOWLEDGEMENT

The authors sincerely wish to thank Mr. H. Hotta, a graduate student of Tokai University, for conducting the experiments and helping them to prepare this paper.

REFERENCES

1. Ando, S.: "On the Hydrodynamic Forces of Mooring Wire Ropes and Chains.", (Part 1: Partial Models), (in Japanese), Trans. West-Japan Soc. Naval Arch., No. 50 (1975)

2. Walton, J.S. and Polachek, H.: "Calculation of Transient Motions of Submerged Cables", Mathematics of Computation, Vol. xiv (1959)

3. Nakajima, T., Motora, S. and Fujino, M.: "On the Study of the Multi-Component Mooring Lines.", (in Japanese). The 5 th Symposium of Ocean Engineering, Soc. of Naval Arch. of Japan (1981)

4. Tsai, N.: "Analysis of a Free-Fall Anchoring Systems.", O.T.C. Paper 1501 (1971)

5. Nakajima, T.: "A Study of the Mooring Dynamics of Various Types by Lumped Mass Method.", (in Japanese) Ph. D Thesis, Univ. of Tokyo (1981)

6. Ando, S. and Kato, S.: "Static and Dynamic Characteristics of Mooring line by chains.", (in Japanese), Abstract Note of the 38 th General Meeting of S.R.I., Ship Research Institute (1981)

7. Nakajima, T., Motora, S. and Fujino, M.: "On the Dynamic Responses of the Moored Object and the Mooring Lines in Regular Waves.", (in Japanese), Trans. Soc. of Naval Arch. of Japan, No. 150 (1981)

APPENDIX

The correction of the weight of line segment is necessary to prevent unrealistic impact load of line from being caused by a drastic change of weight in case where a lumped mass nearest to the bottom hit the bottom or is lifted up from the bottom. In order to prevent the unrealistic impact, a part of the mooring line close to the bottom is approximated by a parabola and the weight of a fraction of the parabola which locates below the bottom surface is neglected (See Fig. 1).

According to this approximation, the weights of the lumped mass nearest to the bottom, that is to say δ_I and that of the next lumped mass, δ_{I+1} are corrected in the following manner:

(1) $0 \leq \Delta\ell_{I-1} < \ell_{I-1}$

$$\delta_I = 1.5\, W_c\, (1. - \Delta\ell_{I-1}/\ell_{I-1})$$

$$\delta_{I+1} = W_c\, (1. + 0.5\, \Delta\ell_{I-1}/\ell_{I-1})$$

where

$$\Delta\ell_{I-1} = - a_{I-1}/b_{I-1}$$

$$a_{I-1} = \frac{x_{I+1}\cdot z_I - x_I\cdot z_{I+1}}{x_I\cdot x_{I+1}\,(x_I - x_{I+1})}$$

$$b_{I-1} = \frac{x_I^2\cdot z_{I+1} - x_{I+1}^2\cdot z_I}{x_I\cdot x_{I+1}\,(x_I - x_{I+1})}$$

$$\ell_{I-1} = \bar{\ell}\, (1. + T_{I-1}/A\cdot E)$$

(2) $\Delta\ell_{I-1} < 0$

$$\delta_I = 1.5\, W_c \quad \text{and} \quad \delta_{I+1} = W_c$$

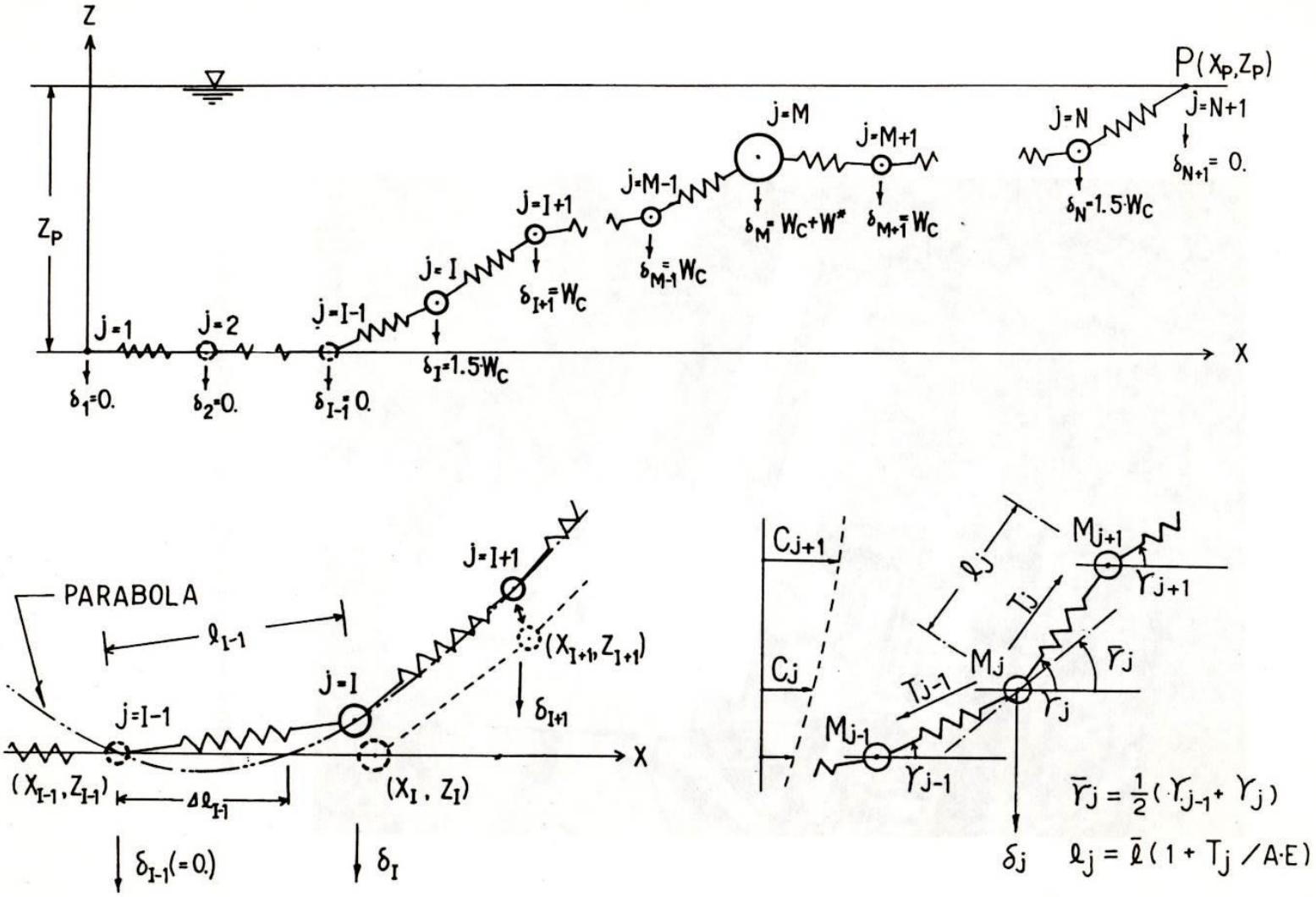

Fig. 1 — Coordinate systems of the lumped mass model

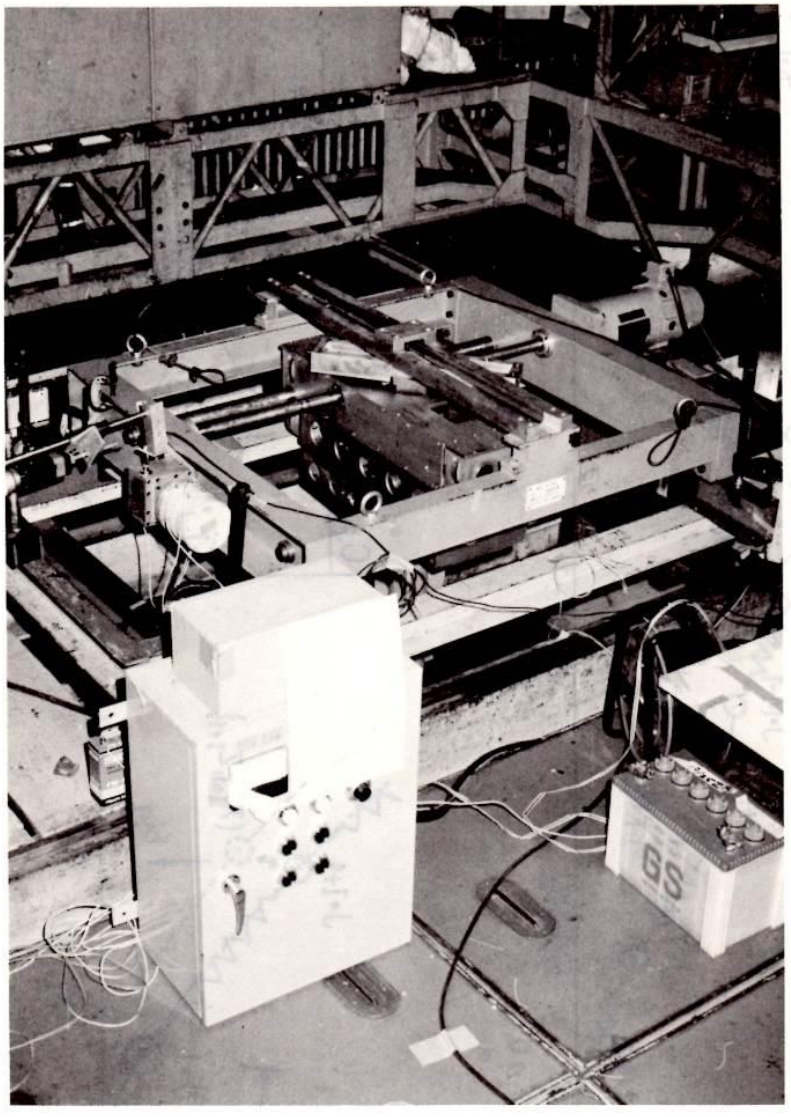

Photo 1 — Apparatus of mechanical forced oscillator

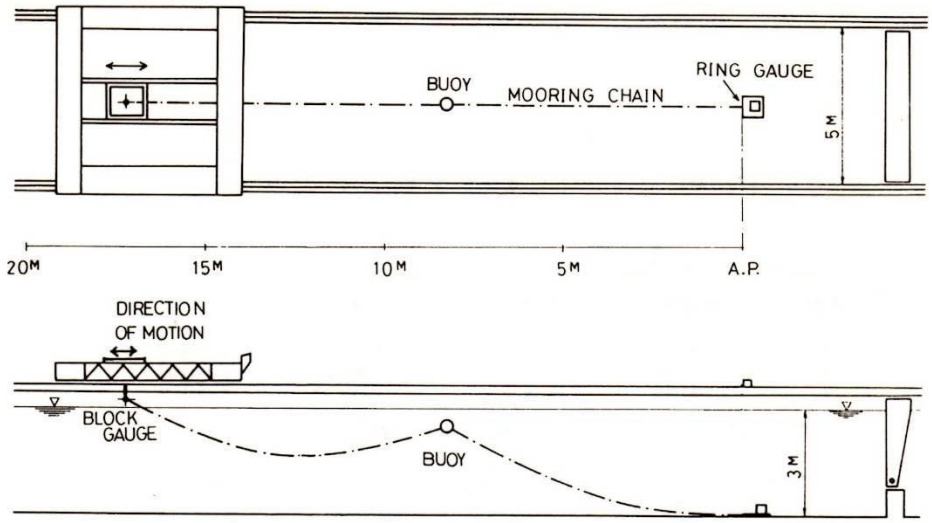

Fig. 2 — Test apparatus of mooring line

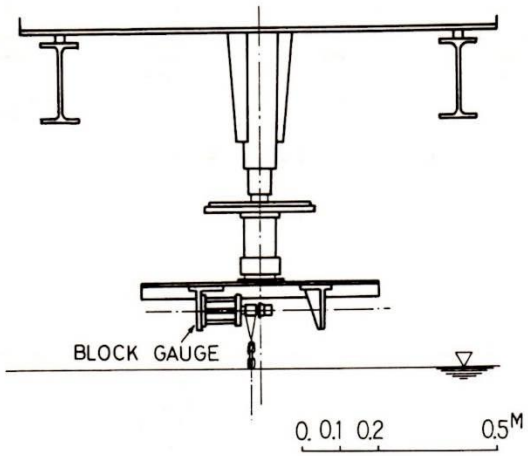

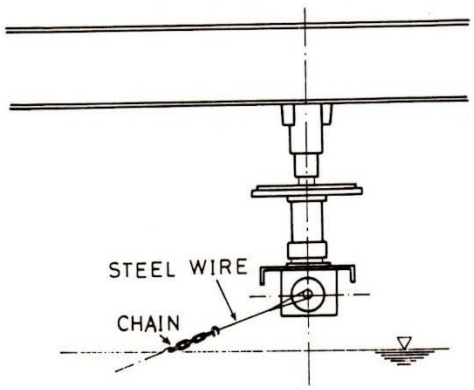

Fig. 3 — Upper end of mooring line

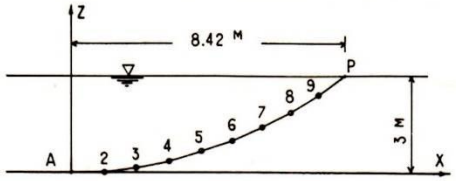

ID No.	Tension(Kg)	Angle(deg.)	x(M)	z(M)
1	2.5391082	0.8971394	0.0000000	0.0000000
4	2.6445727	16.2596529	3.0021154	0.3605167
7	2.8712229	27.8441336	5.8431810	1.4093504
9	3.1363702	35.9558410	7.6015360	2.4063136

A) CONVENTIONAL SINGLE MOORING LINE

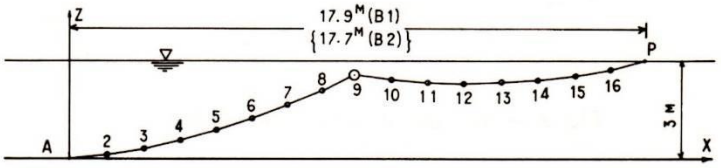

ID No.	Tension(Kg)	Angle(deg.)	x(M)	z(M)
1	4.5956123	5.8201618	0.0000000	0.0000000
5	4.8088027	18.0585451	4.5066253	0.8768454
9	4.6109334	-7.4583730	8.7731644	2.5821370
13	4.5825744	3.9073754	13.3589091	2.3251757
16	4.7045563	13.6373945	16.7824205	2.7288570

B) MOORING LINE WITH SPRING BUOY (B1)

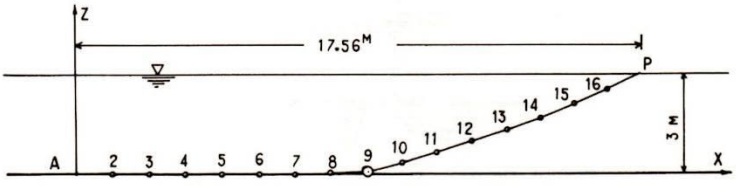

ID No.	Tension(Kg)	Angle(deg.)	x(M)	z(M)
1	9.3994392	0.0000000	0.0000000	0.0000000
5	9.3994392	0.0000000	4.5250015	0.0000000
9	9.7451230	15.3064917	9.0491267	0.0569110
13	10.0189763	20.2545844	13.3708716	1.3933476
16	10.3166257	24.3427090	16.5293184	2.6337060

C) MOORING LINE WITH CLUMP WEIGHT

Fig. 4 — Static configurations of single and multi-component mooring lines

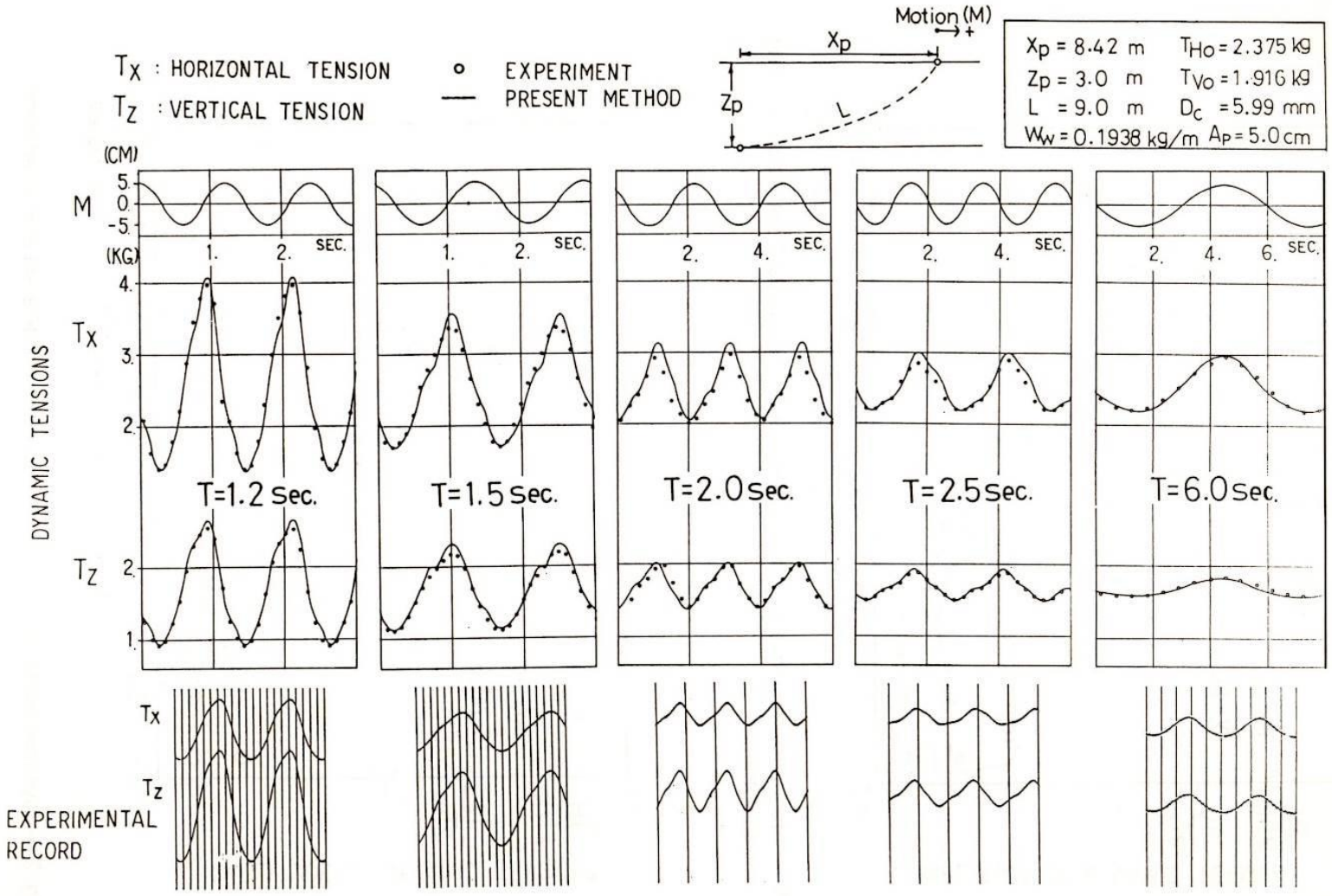

Fig. 5 — Time histories of dynamic tensions obtained by computer simulation (conventional single mooring chain)

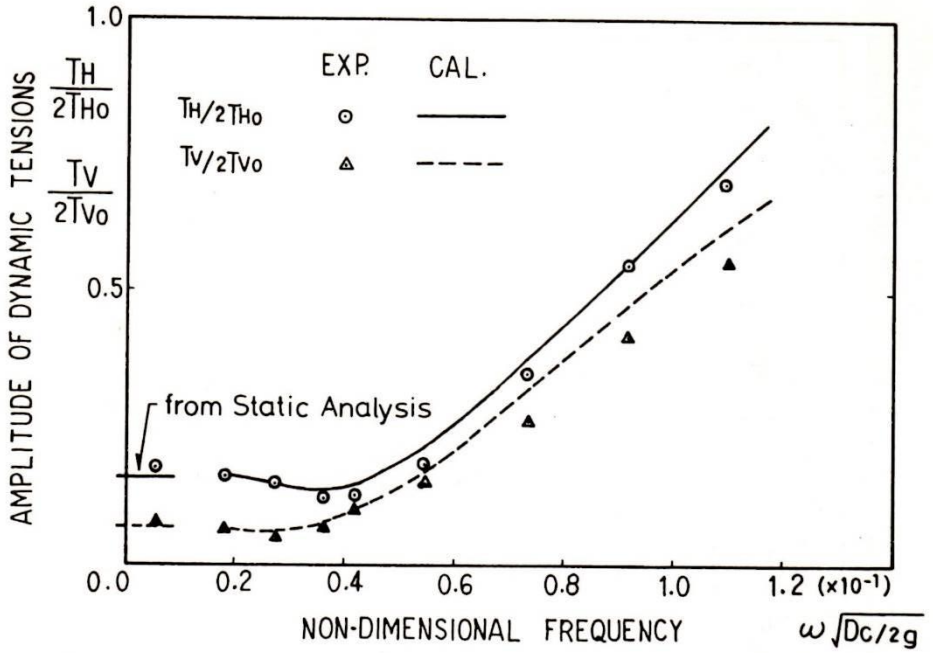

Fig. 6 — Frequency response curves of dynamic tensions (conventional single mooring chain)

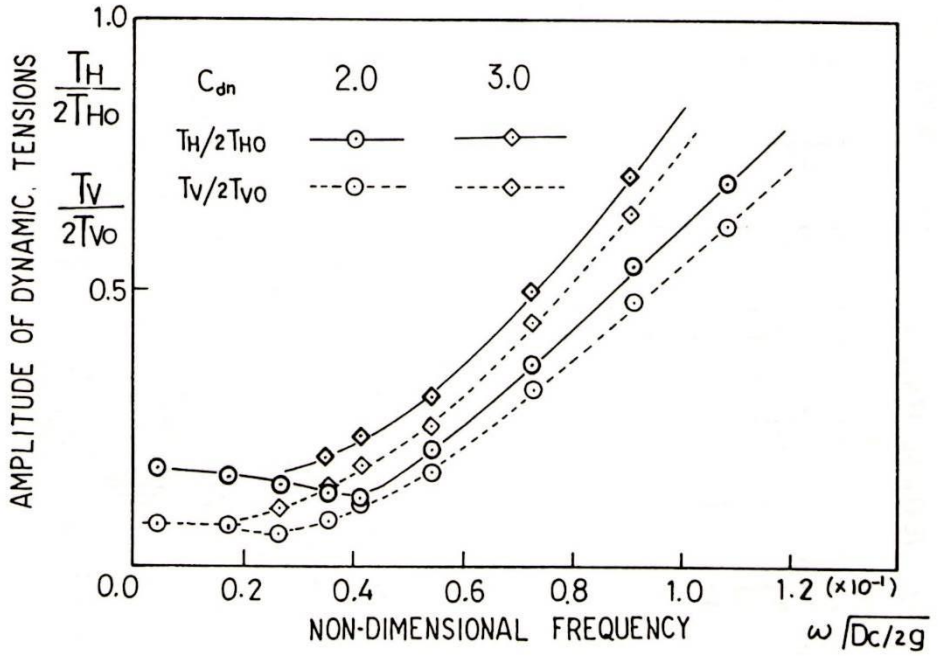

Fig. 7 — Dynamic tensions of single mooring chains of different drag coefficient

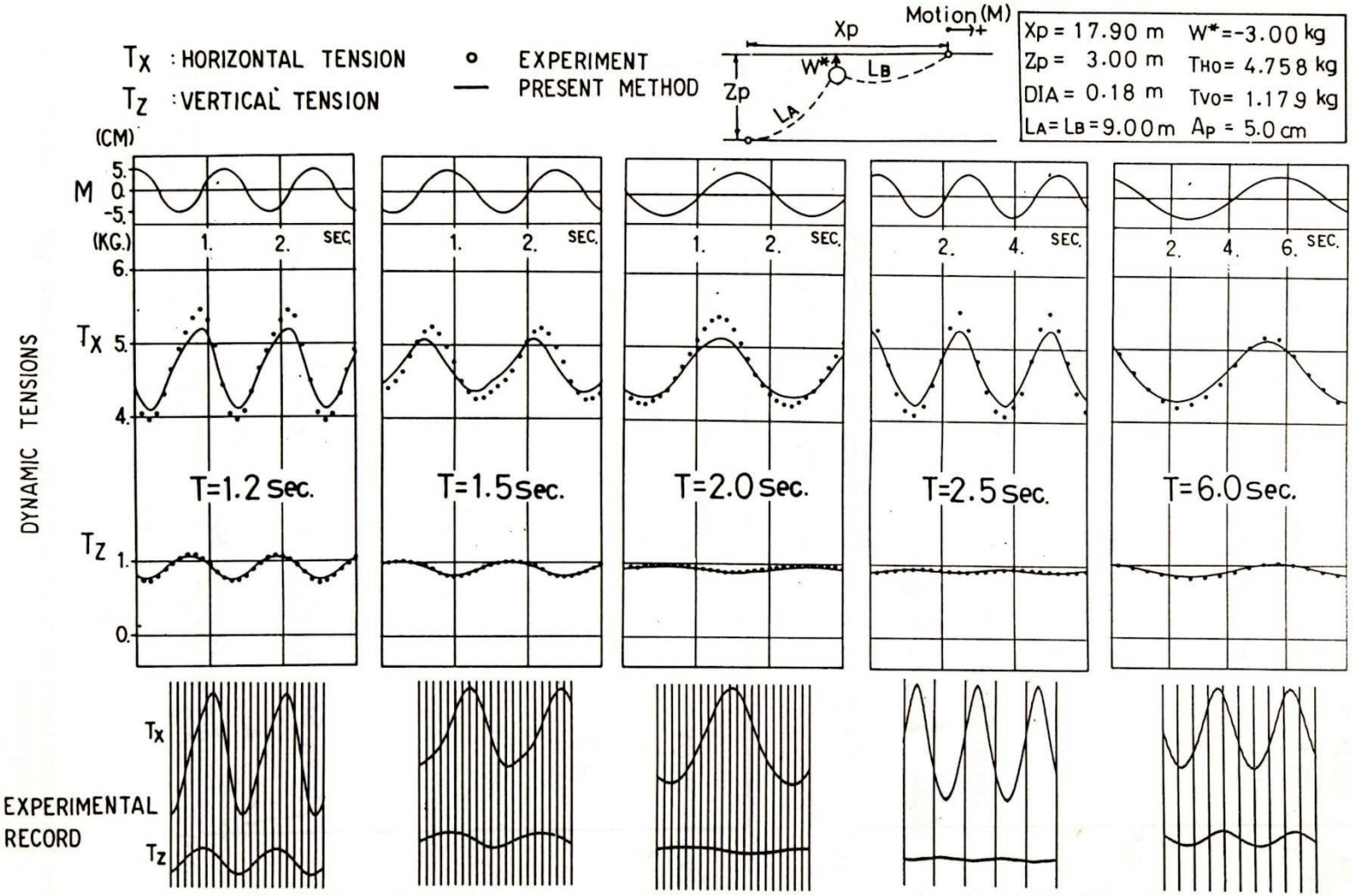

Fig. 8 — Time histories of dynamic tensions obtained by computer simulation (mooring chain with B1 spring buoy)

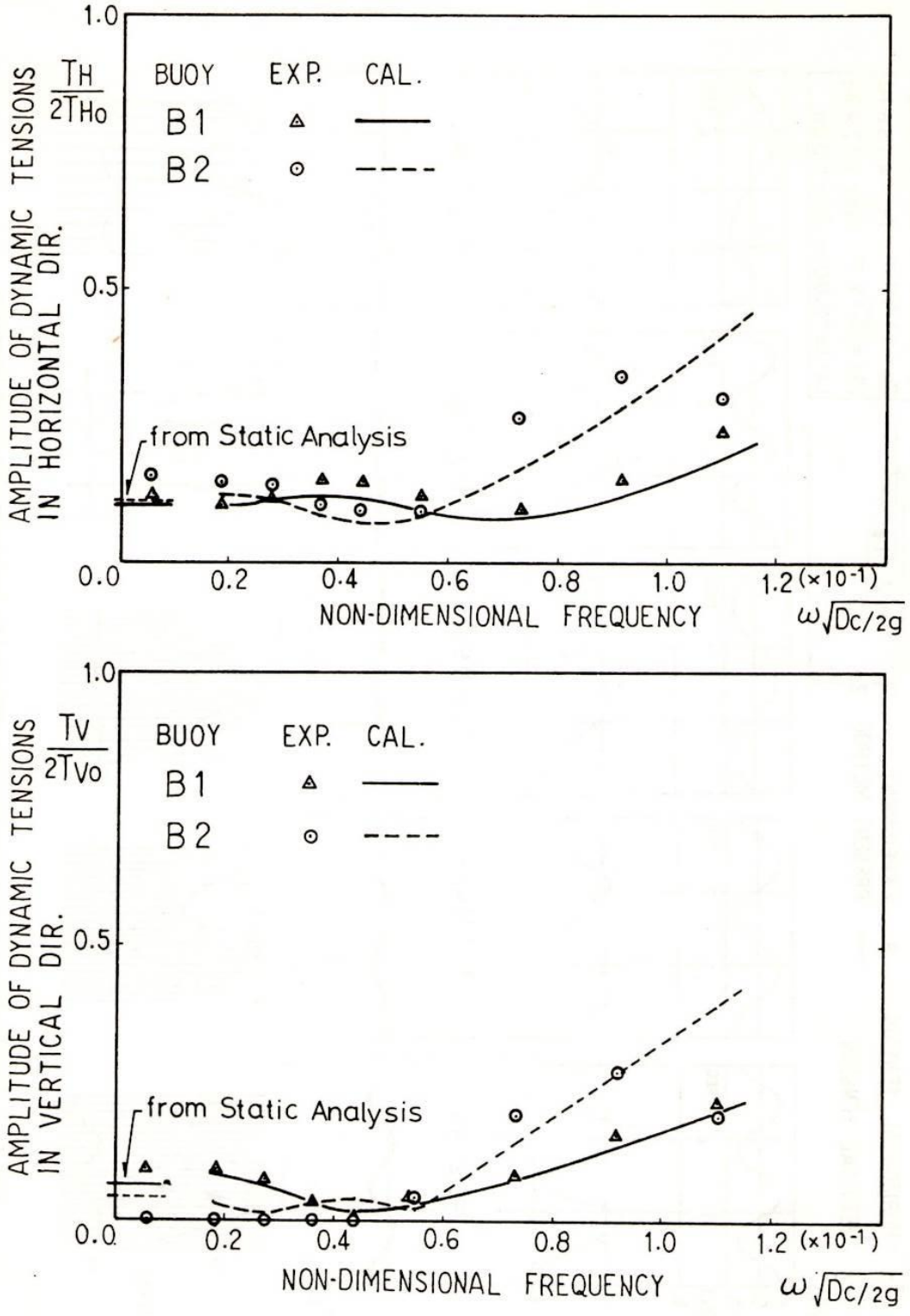

Fig. 9 — Frequency response curves of dynamic tensions (mooring chains with B1 and B2 spring buoys)

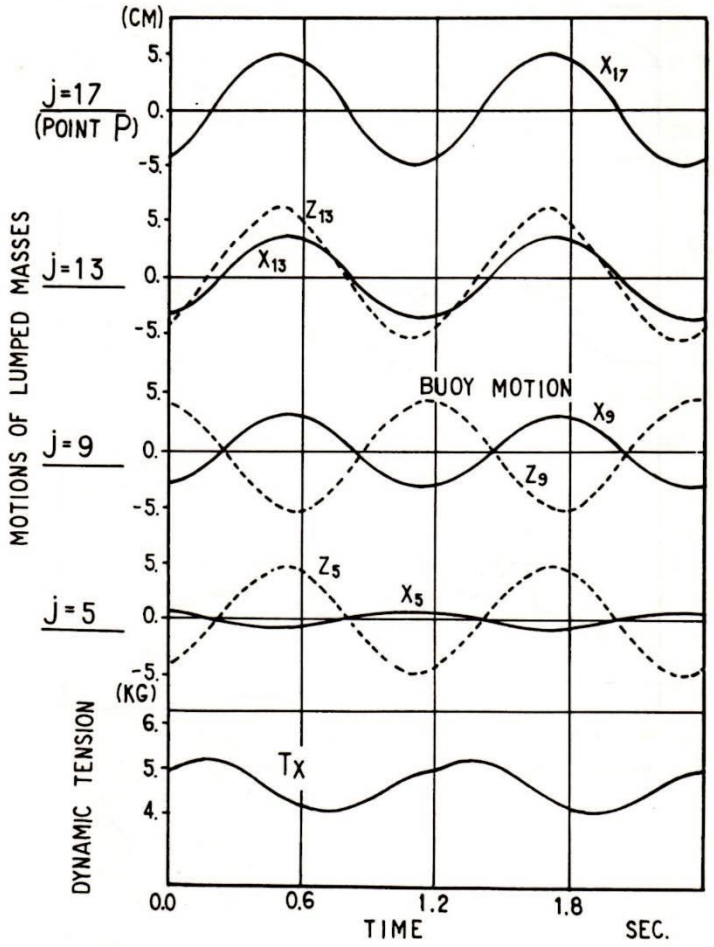

Fig. 10 — Dynamic behaviors of mooring line with B1 spring buoy (period of motion = 1.2 sec, amplitude of motion = 5 cm)

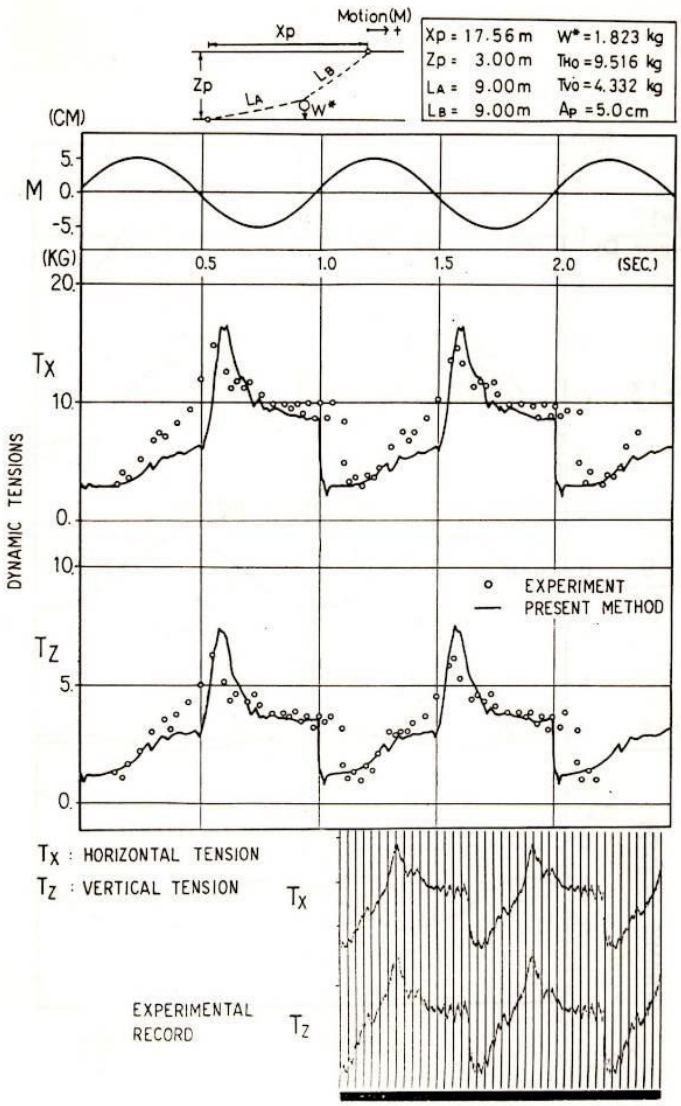

Fig. 11 — Time histories of dynamic tensions obtained by computer simulation (mooring chain with clump weight)